

Multifractality in time series is due to temporal correlations

Jarosław Kwapien^{1,*}, Paweł Blasiak^{1,2,†}, Stanisław Drożdż^{1,3,‡} and Paweł Oświecimka^{1,4,§}

¹*Complex Systems Theory Department, Institute of Nuclear Physics,*

Polish Academy of Sciences, ul. Radzikowskiego 152, 31-342 Kraków, Poland

²*Institute for Quantum Studies, Chapman University, Orange, CA 92866, USA*

³*Faculty of Computer Science and Telecommunications,*

Cracow University of Technology, ul. Warszawska 24, 31-155 Kraków, Poland and

⁴*Faculty of Physics, Astronomy and Applied Computer Science,*

Jagiellonian University, ul. Łojasiewicza 11, 30-348 Kraków, Poland

(Dated: 3 listopada 2022)

Based on the rigorous mathematical arguments formulated within the Multifractal Detrended Fluctuation Analysis (MFDFA) approach it is shown that in the uncorrelated time series the effects resembling multifractality asymptotically disappear when the length of time series increases. The related effects are also illustrated by numerical simulations. This documents that the genuine multifractality in time series may only result from the long-range temporal correlations and the fatter distribution tails of fluctuations may broaden the width of singularity spectrum only when such correlations are present. The frequently asked question of what makes multifractality in time series - temporal correlations or broad distribution tails - is thus ill posed.

I. INTRODUCTION

Multifractality [1–3] is a concept that allows to compactly grasp the most essential aspects of complexity [4] and it therefore pervades all the science. Indeed, its applications cover a broad range of spatial static structures or dynamical phenomena as represented by the time series $x(t)$ [5–17]. The most frequently employed related formal quantitative tool is the multifractal spectrum $f(\alpha)$ which reflects the value of fractal dimension of the support in t of the set of singularities of $x(t)$ carrying a particular value of the Hölder exponents α at the point t [18, 19]. Value of such an exponent reflects the degree of singularity that a fluctuation of $x(t)$ develops at this particular point. The degree of such a singularity is determined by the amplitude of the related fluctuation but also by the amplitudes of fluctuations in its direct neighborhood and such a correspondence cascades through a sequence of scales. The relative ordering of fluctuations, thus the correlations among them, is as important as their absolute values. The related factors are indecomposable and correlations are nonlinear. It is thus seriously surprising that in the scientific literature still a question is being asked as to which factor makes multifractality with correlations and distributions of fluctuations considered as its two independent ‘sources’. In majority of such cases the series are randomly shuffled which of course destroys correlations. The finite width of the multifractal spectrum obtained after such a procedure - thus in the absence of temporal correlations - is then often taken as an evidence that in that particular case multifractality is due to the broadness of tails in the distribution of fluctuations.

Those however are finite size effects - thus a ‘measurement error’ - and they disappear for sufficiently long series. Some numerical and empirical evidence for such effects can be found in [20–25]. The present contribution documents this fact using analytical arguments as well as some corresponding numerical illustrations.

II. FORMAL ARGUMENTS

The algorithm used most frequently for quantifying multifractality in time series is based on detrending [26] and is commonly known as Multifractal Detrended Fluctuation Analysis (MFDFA) [27]. Indeed, this algorithm appears the most stable and practical for such a purpose [28]. Its most general extension that even allows for quantification of the multifractal cross-correlations [29] between two time series in its consistent variant is known as Multifractal Cross-Correlation Analysis (MFCCA) [30] and MFDFA is then its special case.

A. Multifractal detrended cross-correlation analysis (MFCCA)

Let us thus assume there are two time series consisting of T data points: $U = \{u_i\}_{i=1}^T$ and $W = \{w_i\}_{i=1}^T$. As the first step of the procedure, for a given temporal scale s ($s_{\min} \leq s \leq s_{\max}$), the time series is divided into segments of length s by starting from both ends, which brings $M_s = 2\lfloor T/s \rfloor$ segments total, where $\lfloor \cdot \rfloor$ denotes floor equal to integer part in this case. Within each segment ν ($\nu = 0, \dots, M_s - 1$) detrended signal profiles X and Y are constructed by integrating the data points and subtracting a local trend represented by a fitted m th-degree

* jaroslaw.kwapien@ifj.edu.pl

† pawel.blasiak@ifj.edu.pl

‡ stanislaw.drozd@ifj.edu.pl

§ pawel.oswiecimka@ifj.edu.pl

polynomial $P_{z,\nu}^{(m)}(i)$:

$$X_i(s, \nu) = \sum_{j=1}^i u_{j+\nu s} - P_{X,\nu}^{(m)}(i), \quad (1)$$

$$Y_i(s, \nu) = \sum_{j=1}^i w_{j+\nu s} - P_{Y,\nu}^{(m)}(i). \quad (2)$$

Next in each segment a respective covariance between X and Y is calculated:

$$f_{XY}^2(s, \nu) = \frac{1}{s} \sum_{i=1}^s X_i(s, \nu) Y_i(s, \nu). \quad (3)$$

and then the so-defined covariances are used to derive a family of fluctuation functions $F_r^{XY}(s)$ of order r :

$$F_r^{XY}(s) = \left\{ \frac{1}{M_s} \sum_{\nu=0}^{M_s-1} \text{sgn} [f_{XY}^2(s, \nu)] |f_{XY}^2(s, \nu)|^{r/2} \right\}^{1/r}, \quad (4)$$

where $\text{sgn}(x)$ denotes sign of x . Factoring out the covariance sign is needed to prevent the expression becoming complex and to preserve information stored in f_{XY}^2 [30]. The fluctuation functions are calculated for a range of different temporal scales s , with typical s_{\min} larger than the longest sequence of constant signal values and s_{\max} equal to $T/5$ [28].

The fluctuation functions constitute the basic quantities for detecting the fractal properties of time series,

because, if this is the case, one obtains their power-law dependence on scale:

$$F_r^{XY}(s) \sim s^{h(r)}. \quad (5)$$

A family of thus obtained generalized Hurst exponents $h(r)$ can serve as an indicator of the degree of multifractality. When $h(r) = \text{const}$ the structure is just monofractal. Otherwise it is multifractal and the broadness of $h(r)$ -dependence on r reflects the richness of the convolution of various fractal components in forming the resulting multifractal composition.

B. Gaussian uncorrelated signals

We consider the signal profiles X and Y that do not possess any temporal correlations, neither auto- nor cross- and they are described by the same probability distribution. Without loss of generality, let us also assume that $r = 2n$ with $n \in \mathbb{N}$ in order to simplify the calculations (since $h(r)$ is monotonous in r , all non-integer values of the exponent r provide us with $h(r)$ that is placed between its values for the nearest integers).

We intend to work out an analytical assessment of $F_{2n}^{XY}(s)$ for X, Y . We thus start by rewriting Eq.(4) for $r/2 = n$, which allows us to remove the factorization into sign and modulus of f_{XY}^2 :

$$\begin{aligned} [F_{2n}^{XY}(s)]^{2n} &= \frac{1}{M_s} \sum_{\nu=0}^{M_s-1} \left[\frac{1}{s} \sum_{i=1}^s X_i(s, \nu) Y_i(s, \nu) \right]^n = \\ &= \frac{1}{s^n} \sum_{i_1=1}^s \cdots \sum_{i_n=1}^s \frac{1}{M_s} \sum_{\nu=0}^{M_s-1} X_{i_1}(s, \nu) Y_{i_1}(s, \nu) \cdots X_{i_n}(s, \nu) Y_{i_n}(s, \nu) = \frac{1}{s^n} \sum_{i_1=1}^s \cdots \sum_{i_n=1}^s \mathbb{E}(X_{i_1} Y_{i_1} \cdots X_{i_n} Y_{i_n}), \end{aligned} \quad (6)$$

where the arithmetic average over M_s segments ν is replaced by the corresponding moments $\mathbb{E}(\cdot)$. Under the no-memory assumption of the signals, the products $X_g Y_g$ and $X_h Y_h$ are statistically independent for any $g \neq h$ (with $1 \leq g, h \leq s$), which allows for factorization: $\mathbb{E}(\cdots X_g^{l_g} Y_g^{l_g} \cdots X_h^{l_h} Y_h^{l_h} \cdots) =$

$\mathbb{E}(X_g^{l_g} Y_g^{l_g}) \mathbb{E}(X_h^{l_h} Y_h^{l_h}) \mathbb{E}(\cdots)$, where $0 \leq l_g, l_h \leq n$ and $\sum_h l_h = n$.

This factorization and multiple summation in Eq.(6) allows us to rewrite it by considering a combinatorial problem of partitioning an n -element set \mathcal{S} into k subsets of size $\{l_1, \dots, l_k\}$ with $1 \leq l_p \leq n$ and $\sum_{p=1}^k l_p = n$, provided each element of \mathcal{S} can assume one of s values:

$$\begin{aligned} \frac{1}{s^n} \sum_{i_1=1}^s \cdots \sum_{i_n=1}^s \mathbb{E}(X_{i_1} Y_{i_1} \cdots X_{i_n} Y_{i_n}) &= \\ &= \frac{1}{s^n} \sum_{j_1=0}^n \cdots \sum_{j_n=0}^n \frac{n!}{(1!)^{j_1} \cdots (n!)^{j_n}} \frac{1}{j_1! \cdots j_n!} \prod_{l=0}^{k-1} (s-l) \prod_{m=1}^n \mathbb{E}^{j_m}(X^m Y^m), \end{aligned} \quad (7)$$

where $\sum_m j_m = k$ and $\sum_m m j_m = n$ (with $0 \leq j_m \leq n$). Here we implicitly assumed that the products $X_h Y_h$ have the same probability distribution function for any h , which brought $\mathbb{E}(X_g^m Y_g^m) = \mathbb{E}(X_h^m Y_h^m)$ for any g, h, m . This, in turn, allowed us to neglect the subscripts of X, Y

$$\begin{aligned} S(l_1, \dots, l_k) &= \binom{n}{l_k} \binom{n-l_k}{l_{k-1}} \cdots \binom{n-\sum_{p=2}^k l_p}{l_1} = \frac{n!}{l_k!(n-l_k)!} \frac{(n-l_k)!}{l_{k-1}!(n-l_k-l_{k-1})!} \cdots \frac{(n-\sum_{p=2}^k l_p)!}{l_1!(n-\sum_{p=1}^k l_p)!} = \\ &= \frac{n!}{l_k! l_{k-1}! \cdots l_1!} = \frac{n!}{(1!)^{j_1} \cdots (n!)^{j_n}}, \end{aligned} \quad (8)$$

and writing the last equality in Eq.(8) required a reorganization only ($0 \leq j_p \leq n$). Moreover, since the subsets with the same number of elements should not be distinguishable, we have to divide the final form of $S(l_1, \dots, l_k)$ by $j_1! \cdots j_n!$, which completes the explanation of Eq.(7).

Now we may consider different probability distribution

and led to the product $\prod_l (s-l)$ that is the number of possible n -permutations of s possible g, h values.

The r.h.s. of Eq.(7) comes from a fact that a partition of \mathcal{S} into k subsets of size $\{l_1, \dots, l_k\}$ can be realized in $S(l_1, \dots, l_k)$ ways, where

functions describing the random variables X, Y . A special case is the bivariate Gaussian p.d.f., for which we assume $\mathbb{E}(X) = \mathbb{E}(Y) = 0$ and put $\mathbb{E}(XY) = \sigma_{XY}^2$, $\mathbb{E}(X^2) = \sigma_X^2$, $\mathbb{E}(Y^2) = \sigma_Y^2$. By using the Isserlis theorem [31] generalized to higher-order moments (the well known Wick's probability theorem [32] is its related variant), we write:

$$\mathbb{E}(X^m Y^m) = \sum_{p=0}^{\lfloor m/2 \rfloor} \frac{(m!)^2}{2^{2p} (m-2p)! (2!)^p} \sigma_X^{2p} \sigma_Y^{2p} \sigma_{XY}^{2(m-2p)} = \sum_{p=0}^{\lfloor m/2 \rfloor} \frac{(m!)^2}{2^{3p} (m-2p)!} \sigma_X^{2p} \sigma_Y^{2p} \sigma_{XY}^{2(m-2p)}, \quad (9)$$

where $\lfloor \cdot \rfloor$ denotes integer part. After inserting Eq.(7) and

Eq.(9) into Eq.(6), we obtain a complete form of the r -fluctuation function $F_r^{XY}(s)$:

$$[F_{2n}^{XY}(s)]^{2n} = \frac{1}{s^n} \sum_{j_1=0}^n \cdots \sum_{j_n=0}^n \frac{n!}{(1!)^{j_1} \cdots (n!)^{j_n}} \frac{1}{j_1! \cdots j_n!} \prod_{l=0}^{k-1} (s-l) \prod_{m=1}^n \left(\sum_{p=0}^{\lfloor m/2 \rfloor} \frac{(m!)^2}{2^{3p} (m-2p)!} \sigma_X^{2p} \sigma_Y^{2p} \sigma_{XY}^{2(m-2p)} \right)^{j_m}, \quad (10)$$

where $k = \sum_{m=1}^n j_m$. For large $s \gg n$, which is a typical case, we observe that the factor s^{-n} can suppress all the summed terms except for $k = n$, where we obtain a product:

$$\prod_{l=0}^{n-1} (s-l) = s(s-1)\cdots(s-n+1) \sim \mathcal{O}(s^n). \quad (11)$$

In order to write the corresponding expression for the leading term, we observe that in this case $\sum_{i=1}^n j_i = \sum_{i=1}^n i j_i = n$, which is fulfilled only if $i = 1$, $j_1 = n$, and $j_i = 0$ for $i > 1$. Thus, the expression reads

$$[F_{2n}^{XY}(s)]^{2n} = \frac{1}{s^n} \frac{n!}{(1!)^n n!} \prod_{l=0}^{n-1} (s-l) \left(\frac{(1!)^2}{1!} \sigma_{XY}^2 \right)^n = \frac{\sigma_{XY}^{2n}}{s^n} \prod_{l=0}^{n-1} (s-l) \sim \sigma_{XY}^{2n}, \quad (12)$$

where we exploited the fact that $m = 1$ and $\lfloor 1/2 \rfloor = 0$.

The above result is apparently independent of s , but ac-

tually, for the fractal signals without long-term autocorrelations, it is $\sigma_{XY}^2 = \sigma_{XY}^2(s) \sim s$. As a consequence, we obtain $F_{2n}^{XY}(s) \sim (\sigma_{XY}^2)^{1/2} \sim s^{1/2}$, which is independent of n , i.e. the cross-correlations are monofractal, exactly as expected for the series of uncorrelated Gaussian random variables. This result can be generalized to $F_r^{XY}(s)$, $r \in \mathbb{R}$, provided one notes that the generalized Hurst exponents $h(r)$ in Eq.(5) form a monotonic function of r , so $2n - 1 < r < 2n$ implies that $F_{2n-1}^{XY}(s) < F_r^{XY}(s) < F_{2n}^{XY}(s)$. Of course, the special case of $Y = X$ corresponds to the standard MFDFA technique [27] that deals with the correlations described by $F_r(s)$.

C. Heavy-tailed case

From the Gaussian case discussed above, we now move to the case of random variables with p.d.f.s that have heavy tails, but outside the Lévy-stable regime, which is the most frequent case in real-world signals, including the financial ones [4]. Exactly as before, we postulate that the resulting time series do not have any long-term autocorrelations. This assumption allows us to preserve the factorization of moments shown by Eq.(7), but now the Isserlis theorem cannot be applied and therefore the higher-order moments $\mathbb{E}(X^m Y^m)$ cannot be reduced to a combination of the second moment products. Moreover, for such distributions the higher-order moments become the larger, the heavier are the distribution tails. For the random variables with power-law tails, the moments of sufficiently high order become infinite, which forces one to reduce in principle the maximum allowed r in $F_r(s)$. However, in real data there is always some cut-off of the tails, even if they behave as power-law ones for some range of random variable values, and, thus, one may consider a broader range of rs .

If data under consideration present heavy tails with or without cut-off, there is no longer a possibility that the factor $1/s^n$ suppresses all the terms in Eq.(10) except the leading one ($\sim s^n$) shown in Eq.(11). The higher-order moments can become so large that the corresponding terms are not suppressed even if they are proportional to s^{n-1} , s^{n-2} and so on. In such a case, the calculated $F_{2n}^{XY}(s)$ becomes dependent on n , which - for the fractal data - manifests itself via the variable generalized Hurst exponents $h(2n)$ in Eq.(5). In order to overcome this effect, one needs to take a sufficiently large maximum scale s_{\max} that is able to suppress all the moments occurring with s^{n-1} and the remaining terms in Eq.(10).

From this perspective it is clear that the $F_r^{XY}(s)$ dependence on r for the heavy-tailed random variables and the so-implied ‘‘multifractality’’ is only an apparent effect caused by large values of $\mathbb{E}(X^m Y^m)$ that, in turn, are caused by the moments’ weak convergence to their Gaussian counterparts expected from the central limit theorem for the non-Lévy random variables.

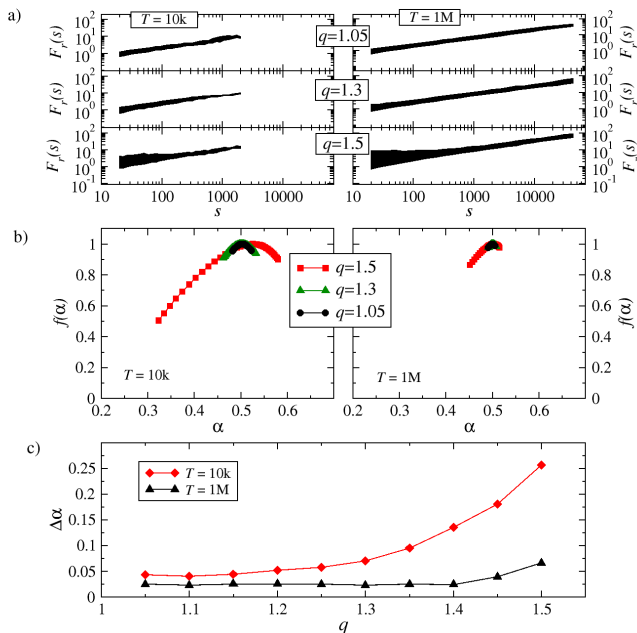
III. NUMERICAL ILLUSTRATIONS

Most often the multifractal characteristics of time series are expressed via the singularity spectrum $f(\alpha) = r[\alpha - h(r)] + 1$, where $\alpha = h(r) + rh'(r)$ is the singularity strength and $h(r)$ is determined by Eq.(5). The degree of multifractality is then measured in terms of the width $\Delta\alpha = \alpha_{\max} - \alpha_{\min}$ between the extreme values of α for an assumed range $r_{\min} \leq r \leq r_{\max}$.

In order to establish an empirical-oriented perspective on the above arguments and to see how the related effects manifest themselves in numerical experiments three model cases are now presented. The first one (i) considers the uncorrelated time series drawn from the q Gaussian distribution,

$$p(x) \sim e_q^{-a_q x^2} = 1/[1 + (q-1)a_q x^2]^{1/(q-1)} \quad (13)$$

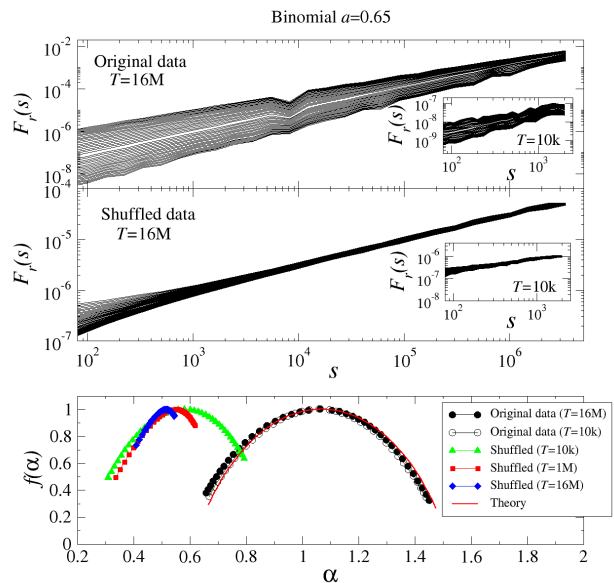
in the scientific literature proposed in connection with the concept of non-extensive entropy [33]. This distribution appears very efficient in reproducing the fluctuations of several natural phenomena including the financial ones [34]. For $q = 1$ it reduces to the standard Gaussian distribution and up to $q = 5/3$ it spans the whole range of heavy-tailed distributions that belong to the Gaussian basin of attraction. In particular, for $q = 3/2$ it corresponds to the so-called ‘inverse-cubic power-law’ that is obeyed almost universally by the high-frequency return distributions in various financial markets [17]. For the present purpose several sets of the time series of length $T = 10^4$ and $T = 10^6$ are generated in 100 realisations each. In Fig. 1 the explicit results for $q = 1.05$, $q = 1.3$ and $q = 1.5$ for the corresponding fluctuation functions (a) and the resulting singularity spectra (b) are shown. Clearly, as it is consistent with the above formal arguments, the effects that can erroneously be interpreted as multifractality disappear with an increasing length of the series. For the larger values of parameter q , as here of $q = 1.5$, thus for the heavier tails in the distribution of fluctuations, this convergence to the correct, monofractal result is very slow, indeed, and the ‘broom’ seen at the smaller values of s can confusingly be interpreted in terms of multifractality. More systematically, these effects of convergence in terms of the width $\Delta\alpha$ of singularity spectrum are illustrated in the panel (c) of Fig. 1. As one can see here, an automatic treatment of the numerical procedure of extracting the singularity spectra from the fluctuation functions $F_r(s)$ for the uncorrelated series of $T = 10^4$ order long at the larger values of q produces sizeable values of $\Delta\alpha$. In order to suppress such artifacts the length of the series needs to reach the orders of $T = 10^6$ especially for q approaching $3/2$. Not shown here, systematically more smeared out is the situation at even larger values of q , those approaching the Lévy-stable basin of attraction that begins at $q = 5/3$. As it is known from analytical considerations [35], the singularity spectrum of uncorrelated series drawn from the Lévy-stable regime assumes a bifractal form. Thus, in numerical realizations, this bifractality is already felt



Rysunek 1. (a) Fluctuation functions $F_r(s)$ (MF DFA) calculated for the signals of length $T = 10^4$ (left) and $T = 10^6$ (right) sampled from three different q Gaussians. In each panel $F_r(s)$ for different moments indexed by $r \in [-4, 4]$ is displayed. (b) The corresponding singularity spectra $f(\alpha)$ as a function of q within the range $1.05 < q < 1.5$.

when q approaches $5/3$, which of course should not be confused with genuine multifractality.

The second (ii) numerical example begins with a correlated series, which by construction is multifractal [27]. A convenient choice is a binomial cascade. Thus a series $\{x_i\}_{i=1}^T$ of length $T = 2^{k_{\max}}$ is generated such that, after k_{\max} steps of iteration, $x_i = a^{n(i-1)}(1-a)^{k_{\max}-n(i-1)}$, where $0.5 < a < 1$ and $n(i)$ denotes the number of unities in the binary representation of i . For $a = 0.65$, a series of length $T = 2^{24}$ (k_{\max}) is generated and numerically inspected using the MF DFA algorithm. The results for different lengths N are shown in Fig. 2. Interestingly, for the original correlated case, either short ($T = 10^4$) or long ($T = 16 \times 10^6$) series lead to essentially the same singularity spectrum. This confirms correctness of the procedure and, in fact, can be anticipated. The genuine multifractality implies self-similarity, thus a portion of the signal encodes already the generator which makes the whole. It should also be noticed that both results agree well with the theoretical predictions [27]. The randomly shuffled variant of the same series, thus without any correlations, changes the picture dramatically. Clearly, the MF DFA-obtained shapes of the singularity spectra are getting narrower with their increasing length as expected based of the formal arguments presented above. The convergence to the correct result of monofractality is very slow and even for the series as long as $T = 10^6$ it still develops a non-zero width.

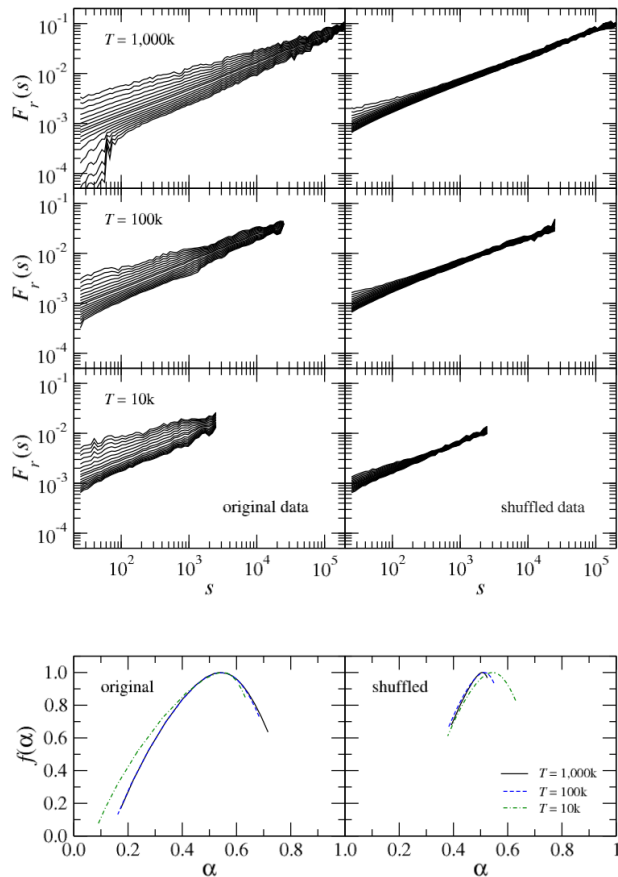


Rysunek 2. (Upper) Fluctuation functions $F_r(s)$ (MF DFA) calculated for the signals generated by the deterministic binomial cascade $a = 0.65$ of length $T = 16 \cdot 10^6$ (upper main panels) and for its shuffled variant (lower main panel). Analogous quantities for $T = 10^4$ are shown in the corresponding insets. The resulting singularity spectra $f(\alpha)$ for the series of length $T = 10^4$ and $T = 16 \cdot 10^6$ correspond to the ones located on the right hand side of the lower panel while their shuffled variant is located on the left hand side of this panel. Here, in addition, the case of $T = 10^6$ is shown.

As a final example (iii) the same multifractality-related characteristics of the real world series representing high-frequency bitcoin price changes are illustrated in Fig. 3. This time series (available from Kraken [36]) represents 1-min price returns covering the period June 21, 2019 — May 15 2021 and comprises over 1 million data points. The shape of the singularity spectrum calculated for this time series is seen to resemble the known cases from the conventional financial markets [15] and, just as for the binomial cascade studied above, the result obtained from the long series ($T \sim 10^6$) is similar to the one obtained already for $T \sim 10^4$. Shuffling destroys the temporal correlations and then, as before, a really long series is needed to approach the monofractal limit.

IV. SUMMARY

Multifractality is a concept that serves efficiently encompassing the nonlinear features of hierarchical organization in complex temporal and spatial structures. In time series the multifractal formalism quantifies the fractal dimension of the support carrying specific values of the Hölder exponents (α) and any such an exponent at a particular point in time series is defined relative to the



Rysunek 3. MFDDFA multifractal characteristics based on over 1 million 1 minute bitcoin returns expressed in USD from the period June 21, 2019 - May 15, 2021 downloaded from Kraken [36], calculated for the original signal samples (left side panels) and for their randomized variants (right side panels) of length $T = 10^4$, $T = 10^5$ and $T = 10^6$ within $r \in [-4, 4]$ moments. Fluctuation functions $F_r(s)$ are shown in the upper panels and the corresponding singularity spectra $f(\alpha)$ are displayed in the lower panels, respectively.

neighbouring values. Therefore, it carries a potential of reflecting the nonlinear principles of the underlying hierarchical organization. Once the time series is randomized by shuffling all the related correlations are expected to get destroyed - at the first place the nonlinear ones - the neighbourhood becomes random and all the Hölder exponents are expected to approach 0.5 (the uncorrelated, trivially monofractal white noise). Of course, for a finite time series, some related dispersion of their values at around 0.5 is natural and this is what typically takes place in numerical analyses. As it is shown in the present contribution, it carries no information at all and is an artifact of the finiteness of the time series. To eliminate such an artifact, the length of the time series needs to approach even millions of data points, especially when the distribution tails are significantly thicker than the Gaussian ones. Numerically, similar effects are observed when the wavelet based algorithms are used (see e.g. Fig. 2 in ref. [21]). On the other hand, once present, the global features of genuine multifractality are encoded already in a relatively short portion of the whole signal as the above numerical experiments document it.

-
- [1] B.B. Mandelbrot, *The Fractal Geometry of Nature* (W. H. Freeman, New York 1982) pp. 373–381.
 - [2] H.E. Stanley and P. Meakin, Multifractal phenomena in physics and chemistry, *Nature* **335**, 405–409 (1988).
 - [3] A. Barabasi and T. Vicsek, Multifractality of self-affine fractals, *Phys. Rev. A* **41**, 2730 (1991).
 - [4] J. Kwapien and S. Drożdż, Physical approach to complex systems, *Phys. Rep.* **515**, 115–226 (2012).
 - [5] A. Rosas, E. Nogueira Jr., and J.F. Fontanari, Multifractal analysis of DNA walks and trails, *Phys. Rev. E* **66**, 061906 (2002).
 - [6] Z.R. Struzik and A.P.J.M. Siebes, Wavelet transform based multifractal formalism in outlier detection and localisation for financial time series, *Physica A* **309**, 388–402 (2002).
 - [7] J.S. Gagnon, S. Lovejoy and D. Schertzer, Multifractal earth topography. *Nonlin. Processes Geophys.* **13**, 541–570 (2006).
 - [8] T. Di Matteo, Multi-scaling in finance, *Quantitative Finance* **7**, 21 (2007).
 - [9] R. Lopes and N. Betrouni, Fractal and multifractal analysis: A review, *Medical Image Analysis* **13**, 634–649 (2009).
 - [10] M. Ausloos, Generalized Hurst exponent and multifractal function of original and translated texts mapped into frequency and length time series, *Phys. Rev. E* **86**, 031108 (2012).
 - [11] S. Dutta, D. Ghosh, and S. Chatterjee, Multifractal detrended fluctuation analysis of human gait diseases, *Front. Physiol.* **4**, 274 (2013).

- [12] S. Drożdż and P. Oświęcimka, Detecting and interpreting distortions in hierarchical organization of complex time series, *Phys. Rev. E* **91**, 030902(R) (2015).
- [13] S. Drożdż, P. Oświęcimka, A. Kulig, J. Kwapien, K. Bazarnik, I. Grabska-Gradzińska, J. Rybicki, and M. Stanuszek, Quantifying origin and character of long-range correlations in narrative texts, *Inf. Sciences* **331**, 32 (2016).
- [14] P. Oświęcimka, L. Livi, and S. Drożdż, Right-side-stretched multifractal spectra indicate small-worldness in networks, *Commun. Nonlinear Sci. Numer. Simul.* **57**, 231 (2018).
- [15] Z.-Q. Jiang, W.-J. Xie, W.-X. Zhou, and D. Sornette, Multifractal analysis of financial markets: a review, *Rep. Prog. Phys.* **82**, 125901 (2019).
- [16] R. Rak, J. Kwapien, P. Oświęcimka, P. Zięba and S. Drożdż, Universal features of mountain ridge networks on Earth, *J. Complex Networks* **8**, cnz017 (2020).
- [17] M. Wątorek, S. Drożdż, J. Kwapien, L. Minati, P. Oświęcimka, and M. Stanuszek, Multiscale characteristics of the emerging global cryptocurrency market. *Phys. Rep.* **901**, 1 (2021).
- [18] T.C. Halsey, M.H. Jensen, L.P. Kadanoff, I. Procaccia, and B.I. Shraiman, Fractal measures and their singularities: The characterization of strange sets, *Phys. Rev. A* **33**, 1141 (1986).
- [19] J.-F. Muzy, E. Bacry, and A. Arneodo, The multifractal formalism revisited with wavelets, *Int. J. Bifurc. Chaos* **4**, 245 (1994).
- [20] J. Kwapien, P. Oświęcimka, and S. Drożdż, Components of multifractality in high-frequency stock returns, *Physica A* **350**, 466 (2005).
- [21] S. Drożdż, J. Kwapien, P. Oświęcimka, and R. Rak, Quantitative features of multifractal subtleties in time series, *EPL* **88**, 60003 (2009).
- [22] W.-X. Zhou, Finite-size effect and the components of multifractality in financial volatility, *Chaos, Solitons & Fractals* **45**, 147 (2012).
- [23] R. Rak and D. Grech, Quantitative approach to multifractality induced by correlations and broad distribution of data, *Physica A* **508**, 48 (2018).
- [24] P. Oświęcimka, S. Drożdż, M. Frasca, R. Gębarowski, N. Yoshimura, L. Zunino, and L. Minati, Wavelet-based discrimination of isolated singularities masquerading as multifractals in detrended fluctuation analyses, *Nonlin. Dyn.* **100**, 1689 (2020).
- [25] F. Olivares and M. Zanin, Corrupted bifractal features in finite uncorrelated power-law distributed data, *Physica A* **603**, 127828 (2022).
- [26] C.K. Peng, S.V. Buldyrev, S. Havlin, M. Simons, H.E. Stanley, and A.L. Goldberger, Mosaic organization of DNA nucleotides, *Phys. Rev. E* **49**, 1685 (1994).
- [27] J.W. Kantelhardt, S.A. Zschiegner, E. Koscielny-Bunde, S. Havlin, A. Bunde, and H.E. Stanley, Multifractal detrended fluctuation analysis of nonstationary time series, *Physica A* **316**, 87 (2002).
- [28] P. Oświęcimka, J. Kwapien, S. Drożdż, Wavelet versus detrended fluctuation analysis of multifractal structures, *Phys. Rev. E* **74**, 016103 (2006).
- [29] W.-X. Zhou, Multifractal detrended cross-correlation analysis for two nonstationary signals, *Phys. Rev. E* **77**, 066211 (2008).
- [30] P. Oświęcimka, S. Drożdż, M. Forczek, S. Jadach, and J. Kwapien, Detrended cross-correlation analysis consistently extended to multifractality, *Phys. Rev. E* **89**, 023305 (2014).
- [31] L. Isserlis, On a formula for the product-moment coefficient of any order of a normal frequency distribution in any number of variables, *Biometrika*. **12**, 134 (1916).
- [32] G.C. Wick, The evaluation of the collision matrix, *Phys. Rev.* **80**, 268 (1950).
- [33] C. Tsallis, Nonadditive entropy and nonextensive statistical mechanics - an overview after 20 years. *Braz. J. Phys.* **39**, 337 (2009).
- [34] R. Rak, S. Drożdż, and J. Kwapien, Nonextensive statistical features of the Polish stock market fluctuations, *Physica A* **374**, 315 (2007).
- [35] H. Nakao, Multi-scaling properties of truncated Lévy flights, *Phys. Lett. A* **266**, 282 (2000).
- [36] Kraken API. Available online: <https://www.kraken.com/features/api>